

# Thermodynamic analysis of a thermoelectric power generator in relation to geometric configuration device pins



Haider Ali, Ahmet Z. Sahin\*, Bekir S. Yilbas

Department of Mechanical Engineering, King Fahd University of Petroleum & Minerals, Dhahran 31261, Saudi Arabia

## ARTICLE INFO

### Article history:

Received 2 October 2013

Accepted 21 November 2013

Available online 18 December 2013

### Keywords:

Thermoelectric

Power

Leg geometry

Efficiency

Exponential area variation

## ABSTRACT

Thermoelectric generators (TEG) are cost effective solid-state devices with low thermal efficiencies. The limitations, due to the operational temperature of the thermoelectric materials, suppress the Carnot efficiency increase of the device. Although thermoelectric generators have considerable advantages over the other renewable energy devices, low convergence efficiency of the device retains thermoelectric devices behind its competitors. In order to keep up with the competition, improvement of device efficiency becomes crucial for the practical applications. The design configuration of the device pin legs, lowering the overall thermal conductance, can improve the device efficiency. Therefore, in the present study, the influence of pin leg geometry on thermal performance of the device is formulated thermodynamically. In this case, the exponential area variation of pin legs is considered and dimensionless geometric parameter 'a' is introduced in analysis. The influence of dimensionless geometric parameter on efficiency and power output is demonstrated for different temperature ratios and external load resistance ratios. It is found that increasing dimensionless geometric parameter improves the thermal efficiency of the device; however, the point of maximum efficiency does not coincide with the point of the maximum device output power.

© 2013 Elsevier Ltd. All rights reserved.

## 1. Introduction

Thermoelectric generators (TEG) are a solid-state, which are used to convert thermal energy into electrical energy. The conversion of waste heat into electricity takes place in the device pins due to the Seebeck effect. A thermoelectric generator (TEG) creates voltage because of charge carriers in semiconductor pins, which are free to move much like gas molecules while carrying charge as well as heat. A potential difference is produced because of the buildup of charge carriers, which result in a net charge at the cold end. Since TEG does not contain any moving part and no require combustion, they can be considered as one of the alternative renewable energy resources. TEG can be used to recover waste heat and convert it into electrical power, which becomes important with awareness of the environmental impact on global climate change. The TEG efficiency depends upon the operating temperature, figure of merit, and design configuration of the device. Geometric configuration of thermoelectric is one of the important factors affecting the thermal efficiency and the power output of thermoelectric generator. Therefore, investigation of geometric configuration of TEG is becomes essential.

Considerable research studies were carried out to examine thermoelectric device performance. Hoder [1] studied the thermoelectric generator characteristics to find the optimum arrangements of semiconductor pellets. He discussed the effect of number of pellets and their heights on the maximum output power and efficiency of the thermoelectric generator. Yilbas and Sahin [2] introduced the dimensionless parameters, namely, slenderness ratio and the external load parameter to maximize the efficiency and the output power of a thermoelectric generator. Their finding revealed that the efficiency attains high values for the slenderness ratio less than 1 for almost all the cases considered in the study. Lavric [3] performed 1-D thermal analysis to investigate the thermoelectric performance with respect to geometry for the practical applications. She concluded that power output depended on two opposite effects including: (i) reduction in the leg length reduces the electric resistance and (ii) larger legs ensured the higher temperature difference between the two ends of the legs. Sahin et al. [4] studied the effect of thermoelectric generator on the performance of the topping cycle. They showed that the overall efficacy of the system increased slightly for some range of operational conditions. The thermoelectric generator performance analysis was carried out by Chen et al. [5]. They considered the fixed number of thermoelectric elements of the combined device in order to optimize the system heat load and the coefficient of performance. They indicated that the location of the thermoelectric device was critical to

\* Corresponding author. Tel.: +966 138602548; fax: +966 138602949.

E-mail address: [azsahin@kfupm.edu.sa](mailto:azsahin@kfupm.edu.sa) (A.Z. Sahin).

**Nomenclature**

$a$	dimensionless geometric parameter	$r_\sigma$	electrical conductivity ratio
$A(x)$	exponential variation of area ( $\text{m}^2$ )	$R$	total electrical resistance ( $\Omega$ )
$A_a$	constant in exponential variation of area ( $\text{m}^2$ )	$R_L$	external load resistance ( $\Omega$ )
$A_H$	area of high temperature side ( $\text{m}^2$ )	$R_o$	reference electrical resistance ( $\Omega$ )
$A_L$	area of low temperature side ( $\text{m}^2$ )	$R_{\text{leg}}$	overall electrical resistance in leg ( $\Omega$ )
$A_0$	area of rectangular geometry of thermoelectric generator ( $\text{m}^2$ )	$T_1$	temperature of hot side (K)
$A_R$	area ratio of high temperature and cold temperature side	$T_2$	temperature of cold side (K)
$I$	electrical current (A)	$V_o$	constant volume of thermoelectric material ( $\text{m}^3$ )
$k$	thermal conductivity (W/m K)	$W$	thermoelectric power generation (W)
$k_n$	thermal conductivity of n-type semi-conductor (W/m K)	$ZT_{\text{avg}}$	dimensionless figure of merit
$k_p$	thermal conductivity of p-type semi-conductor (W/m K)	$\alpha$	total Seebeck coefficient (V/K)
$K$	overall thermal conductivity of the thermoelectric generator (W/K)	$\alpha_p$	seebeck coefficient of p-type semi-conductor (V/K)
$K_o$	reference thermal conductivity for thermoelectric generator (W/K)	$\alpha_n$	seebeck coefficient of n-type semi-conductor (V/K)
$L$	length of leg of thermoelectric generator (m)	$\eta$	efficiency
$\dot{Q}$	rate of heat transfer (W)	$\sigma_p$	electrical conductivity of p-type semi-conductor (S/m)
$r_k$	thermal conductivity ratio	$\sigma_n$	electrical conductivity of n-type semi-conductor (S/m)
		$\theta$	dimensionless temperature = $T_1/T_2$

maximize the efficiency of the heat pumps. Design and thermal analysis of solar thermoelectric power generation system was carried out by Vatcharasathien et al. [6]. They incorporated the truncated parabolic collectors with a flat receiver, conventional flat-plate collectors, and thermoelectric power generator modules in the analysis. The simulation study for the performance analysis of the thermoelectric power generation with multi-panels was carried out by Suzuki and Tanaka [7]. They demonstrated that the proper arrangements of the thermoelectric panels could shorten significantly the device area despite the fact that the output from the multi-panels could decrease a few percent. Gou et al. [8] carried out experimental study for low temperature waste heat thermoelectric system. They developed a mathematical model for the system. They indicated that use of the thermoelectric generator could save energy from the low temperature waste heat system. Amatya and Ram [9] analyzed the thermoelectric generator for practical applications. Thermodynamic analysis was presented to predict the thermal-to-electric conversion efficiency of the generator. Weinberg et al. [10] studied the thermoelectric power conversion from heat re-circulating combustion systems. They found that the efficiency of thermoelectric devices could be improved for certain arrangements of the locations of the devices around the heat transferring surface. Freunek et al. [11] presented a physical model for a thermoelectric generator. They investigated the influence of heating conditions and load resistance on the thermoelectric power generation. Extensive amount of work has been done in literature [12–20] for studying the thermodynamic analysis of thermoelectric devices performance. In some work the influence of the geometric configuration on thermoelectric devices is considered [21–28]. However, the effect of leg geometry on the performance of the thermoelectric generator has received very little attention. In the present study, the theoretical analysis of thermoelectric generator performance is carried out by considering the effects of leg geometry configuration, operating parameters such as temperature ratio, external load and device resistances. One dimensionless geometric parameter is introduced which defines the effects of leg geometry on power output and efficiency of thermoelectric generator. The study is extended to include the effects of the device leg geometry on the maximum output power and the maximum efficiency of the thermoelectric generator. In the process of the performance optimization the volume of the leg

material is kept constant. Thus the geometry of the legs (i.e. the cross sectional area of the legs) is varied by re-distributing the available constant amount of thermoelectric material along the legs of the generator.

## 2. Thermal analysis

Consider the thermoelectric element of variable cross section as shown in Fig. 1. The properties of leg material are assumed to be temperature independent so that the Thomson effect is inherently neglected. After introducing the Dirichlet boundary conditions, the efficiency of the thermoelectric power generator with legs of variable cross-section (Fig. 1), can be written as:

$$\eta = \frac{I^2 R_L}{\alpha I T_1 + K(T_1 - T_2) - \frac{1}{2} I^2 R} \quad (1)$$

where  $K$  is the thermal conductance and  $R$  is the electrical resistivity of the thermoelectric generator. The current  $I$  is a function of the net Seebeck coefficient  $\alpha = \alpha_p - \alpha_n$  (the difference between the Seebeck coefficient of  $p$  and  $n$  junctions), the upper and lower temperature ( $T_1$  and  $T_2$ ), the electrical resistance  $R$  and the external load resistance  $R_L$  as:

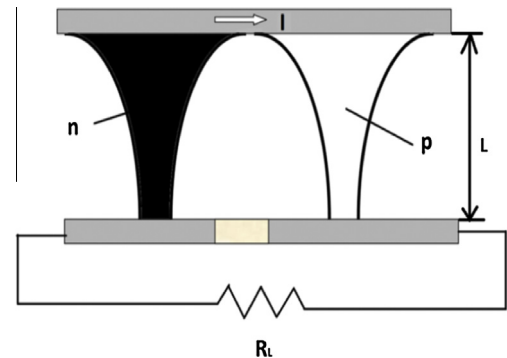


Fig. 1. A schematic view of a thermoelectric power generator with variable cross section legs (pins).

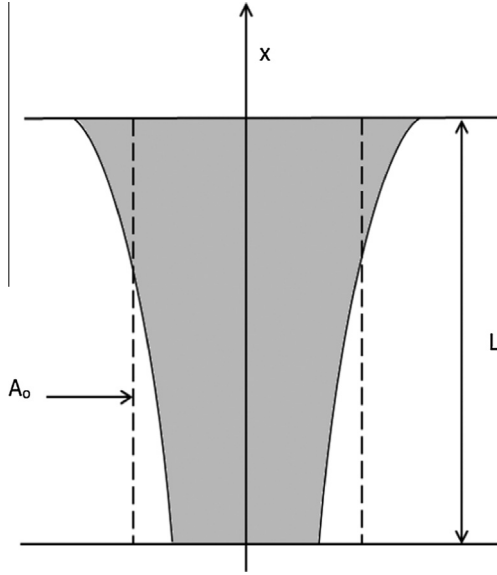


Fig. 2. A schematic view of geometric configuration of thermoelectric generator leg (pin).

$$I = \frac{\alpha(T_1 - T_2)}{R_L + R} \quad (2)$$

Using the definition of  $I$  in Eq. (1), the efficiency becomes:

$$\eta = \frac{\alpha^2(T_1 - T_2)R_L}{K(R_L + R)^2 + \alpha^2 T_1(R_L + R) - \frac{1}{2}\alpha^2(T_1 - T_2)R} \quad (3)$$

The vertical length of both  $p$  and  $n$  type semiconductor of thermoelectric generator is  $L$ . The exponential variation area is considered for both legs (Fig. 2) and it can be defined as:

$$A(x) = A_a e^{(-ax/L)} \quad (4)$$

where  $A_a$  is constant and  $a$  is the dimensionless geometric parameter.  $A_a$  can be obtained through integrating the  $A(x)$  over the length  $L$  and keeping the volume of thermoelectric material kept constant, i.e.:

$$\int_0^L A(x) dx = V_o \quad (5)$$

or

$$A_a \int_0^L e^{(-ax/L)} dx = V_o \quad (6)$$

One can consider that  $V_o = A_0 L$  where  $A_0$  is the area of rectangular geometry cross section area as shown in Fig. 2. After introducing  $V_o$ , the  $A_a$  becomes:

$$A_a = \frac{aA_0}{(1 - e^{-a})} \quad (7)$$

Now using Eq. (7), in Eq. (4) the area  $A(x)$  become:

$$A(x) = \frac{aA_0}{(1 - e^{-a})} e^{(-ax/L)} \quad (8)$$

The rate of heat transfer thorough the leg along  $x$ -axis is given by:

$$\dot{Q} = -kA \frac{dT}{dx} \quad (9)$$

After considering steady heating situation and isolated leg surfaces, Eq. (9) can be written as:

$$\int_0^L \frac{\dot{Q}}{A(x)} dx = -kA \int_{T_1}^{T_2} dT \quad (10)$$

Now after integration heat transfer rate ( $\dot{Q}$ ) becomes:

$$\dot{Q} = \left( \frac{ka^2 A_0}{(e^a + e^{-a} - 2)L} \right) (T_1 - T_2) \quad (11)$$

Eq. (11) indicates that the overall thermal conductance of the leg is:

$$K_{leg} = \frac{ka^2 A_0}{(e^a + e^{-a} - 2)L} \quad (12)$$

Considering the two legs in Fig. 1, the total thermal conductance of the thermoelectric generator can be written as:

$$K = \frac{a^2 (k_n + k_p) A_0}{(e^a + e^{-a} - 2)L} \quad (13)$$

where  $k_n$  and  $k_p$  are the thermal conductivities of  $p$ -type and  $n$ -type legs respectively.

The overall electrical resistance of the leg can be written as:

$$R_{leg} = \int_0^L \frac{dx}{\sigma A(x)} \quad (14)$$

Substituting  $A(x)$  from Eq. (8) and performing the integration, the overall electrical resistance can be obtained as:

$$R_{leg} = \frac{(e^a + e^{-a} - 2)L}{a^2 A_0 \sigma} \quad (15)$$

Similarly, considering the two legs the total electrical resistance of the thermoelectric generator becomes:

$$R = \frac{(e^a + e^{-a} - 2)L}{a^2 A_0} \left( \frac{\sigma_n + \sigma_p}{\sigma_n \sigma_p} \right) \quad (16)$$

where  $\sigma_n$  and  $\sigma_p$  are the electrical conductivities of  $p$ -type and  $n$ -type legs respectively.

Introducing the following dimensionless parameters such as:

Area ratio:

$$A_R = \frac{A_H}{A_L} = e^{-a} \quad (17)$$

Dimensionless figure of merit on the average temperature:

$$ZT_{avg} = \frac{\alpha^2 \left( \frac{\sigma_n}{k_n} \right) T_1}{\left( 1 + \sqrt{\frac{r_k}{r_\sigma}} \right)^2} \left( \frac{1 + \theta}{2} \right) \quad (18)$$

Temperature ratio:

$$\theta = \frac{T_2}{T_1} \quad (19)$$

Thermal conductivity ratio:

$$r_k = \frac{k_p}{k_n} \quad (20)$$

Electrical conductivity ratio:

$$r_\sigma = \frac{\sigma_p}{\sigma_n} \quad (21)$$

Reference thermal conductance

$$K_0 = \frac{A_0 k_n}{L} \quad (22)$$

Reference electrical conductance:

$$R_0 = \frac{L}{A_0 \sigma_n} \quad (23)$$

Dimensionless overall thermal conductance using Eqs. (13), (17), and (22) yields:

$$\frac{K}{K_0} = \frac{a^2(1+r_k)A_R}{(A_R-1)^2} \quad (24)$$

Dimensionless overall thermal conductance using Eqs. (16), (17), and (23) becomes:

$$\frac{R}{R_0} = \frac{(1+r_\sigma)}{r_\sigma} \frac{(A_R-1)^2}{a^2 A_R} \quad (25)$$

Using the dimensionless parameters in Eq. (3), one can get:

$$\eta = \frac{(1-\theta)}{(1+\theta)} \frac{2ZT_{avg} \left(1 + \sqrt{\frac{r_k}{r_\sigma}}\right)^2 \left(\frac{R_L}{R_0}\right)}{\left(\frac{K}{K_0}\right) \left(\frac{R_L}{R_0} + \frac{R}{R_0}\right)^2 + 2ZT_{avg} \left(1 + \sqrt{\frac{r_k}{r_\sigma}}\right)^2 \left(\frac{R_L}{R_0} + \frac{1}{2}(\theta+1)\frac{R}{R_L}\right)} \quad (26)$$

The power generation from the thermoelectric power generation is given as:

$$W = I^2 R_L \quad (27)$$

Using the Eq. (2) i.e. definition of  $I$  in Eq. (27), one can get:

$$W = \frac{\alpha^2(T_1 - T_2)^2 R_L}{(R_L + R)^2} \quad (28)$$

Using the dimensionless parameter the Eq. (28) the dimensionless power generation can be written as:

$$\frac{W}{K_0 T_2} = 2 \frac{(1-\theta)^2}{\theta(1+\theta)} \frac{ZT_{avg} \left(1 + \sqrt{\frac{r_k}{r_\sigma}}\right)^2 \left(\frac{R_L}{R_0}\right)}{\left(\frac{R_L}{R_0} + \frac{R}{R_0}\right)^2} \quad (29)$$

The following material parameters have been used in the analysis as default values to represent practical applications such as skutterudite thermoelectric material:

$$r_k = 1, r_\sigma = 1, \theta = 0.5 \text{ and } ZT_{avg} = 1.5$$

The ranges of operating parameters have been selected to accommodate a wide range of practical situations. Thus the following ranges of operating parameter were considered:

$$0 < \theta < 1.0$$

$$1 < R_L/R_0 < 10$$

$$-8 < a < +8$$

A computer code has been developed using MATLAB to simulate characteristics of thermoelectric generator by varying the geometry of legs (pins).

### 3. Results and discussion

Thermodynamic analysis of thermoelectric power generator is carried out to examine the influence of thermoelectric generator leg geometric configuration on thermal efficiency and output power of the device. The area of thermoelectric generator leg is varied exponentially while keeping the legs height and their volume constant in the formulations. The main purpose of the present work is to show how the performance of the thermoelectric generator can be improved by varying the geometry of the legs without changing the amount of thermoelectric material used in the generator. The height of the generator is also kept constant and therefore the constant amount of the thermoelectric material is distributed in the vertical direction along the legs of the generator in an optimal way so that the performance of the thermoelectric generator possibly becomes the maximum. The geometric parameter “ $a$ ” in Eq. (4) can be varied to obtain different geometries of the thermoelectric generator legs. Parameter  $a = 0$  corresponds to the uniform cross-sectional area legs and the sign (+ or –) in front of the param-

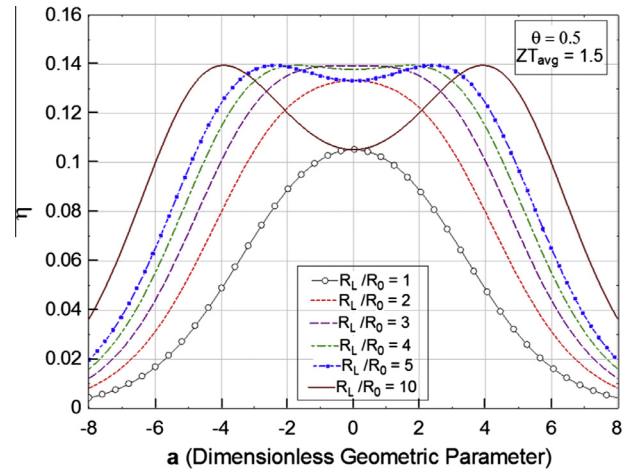


Fig. 3a. Variation of thermal efficiency with dimensionless geometric parameter ( $a$ ) for different values of external load ratio ( $R_L/R_0$ ) and temperature ratio  $\theta = 0.5$ .

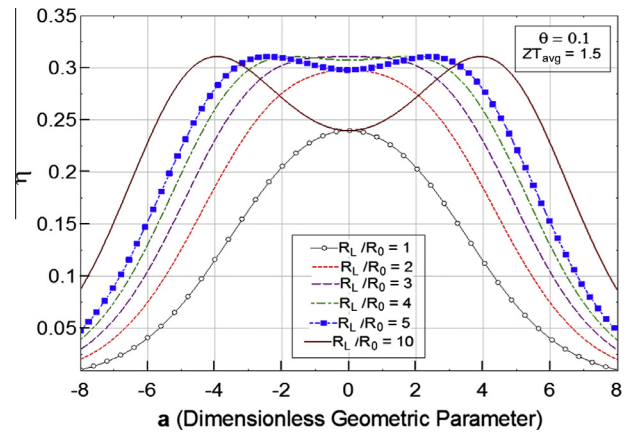


Fig. 3b. Variation of thermal efficiency with dimensionless geometric parameter ( $a$ ) for different values of external load ratio ( $R_L/R_0$ ) and temperature ratio  $\theta = 0.1$ .

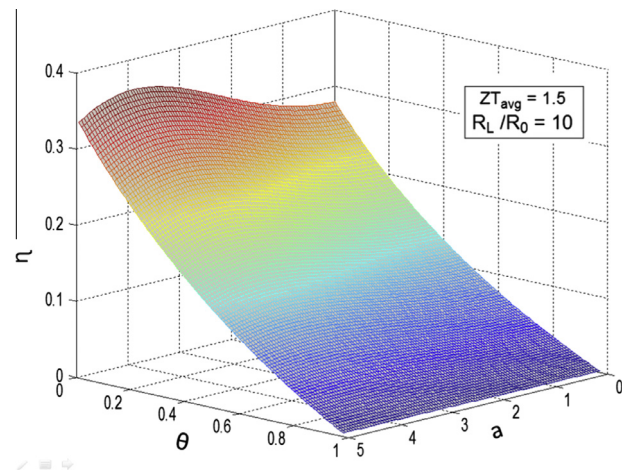


Fig. 4. Three-dimensional view of thermal efficiency variation with dimensionless geometric parameter ( $a$ ) and temperature ratio ( $\theta$ ) for  $R_L/R_0 = 10$ .

eter “ $a$ ” provides increasing or decreasing trend of the cross-sectional area along the legs. Wide range of values for the parameter “ $a$ ” is considered to accommodate variety of practical



cases. Changing the sign of parameter “ $a$ ” simply means turning the pins upside down.

Fig. 3 shows the variation of thermal efficiency with dimensionless geometric parameter ( $a$ ) for different values of external load ratio ( $R_L/R_0$ ) while Fig. 4 shows three-dimensional view of efficiency variation with geometric parameter ( $a$ ) and temperature ratio ( $\theta$ ). The curves behave symmetric along “ $a = 0$ ”. It should be noted that the slope of the leg profile changes for the values of  $a > 0$  and  $a < 0$  (Eq. (8)). As the external load ratio increases, the location of the maximum efficiency shifts towards the small values of dimensionless geometric parameter. This behavior is attributed to non-linear behavior of thermal efficiency with geometric parameter (Eq. (26)). In this case, geometric parameter is incorporated with the leg (pin) resistance (Eq. (16)). Consequently, varying the leg resistance influences thermal efficiency such that efficiency reaches to its maximum when the resistance reduces to its minimum value. However, reducing external load ratio does not influence the maximum value of thermal efficiency, provided that further reduction in external load ratio lowers the maximum value of thermal efficiency, i.e. the values of  $R_L/R_0 < 3$  reduce thermal efficiency considerably. In addition, geometric parameter corresponding to the maximum efficiency remains the same at  $a = 0$  for  $R_L/R_0 < 3$ . This corresponds to the parallel sided legs (pins) of the thermoelectric generator. Therefore, thermoelectric generator operating at external load parameter  $R_L/R_0 < 3$  should have parallel leg configuration. In the case of temperature ratio ( $\theta$ ), the maximum efficiency attains high values at low value of temperature ratio. Increase in thermal efficiency is associated with increasing Carnot efficiency of the thermoelectric device. Therefore, increased Carnot efficiency improves the maximum efficiency of the thermoelectric generator. Temperature ratio does not influence the behavior of thermal efficiency variation with geometric parameter ( $a$ ), except the values of thermal efficiency changes. Consequently, thermal efficiency of the thermoelectric generator improves significantly with modifying leg geometry. This is true for high values of external load ratio, which is more pronounced for low values of temperature ratio. It can be observed from Fig. 3 that reducing temperature ratio increases the maximum value of thermal efficiency and the corresponding value of geometric leg parameter changes with varying temperature ratio. Fig. 5 also shows variation of thermal efficiency with temperature ratio for external load ratio  $R_L/R_0 = 10$  and geometric leg parameter  $a = 3.99$  at which the maximum thermal efficiency occurs. Thermal efficiency decreases with increasing temperature ratio and this decrease is in a nonlinear form (Eq. (24)).

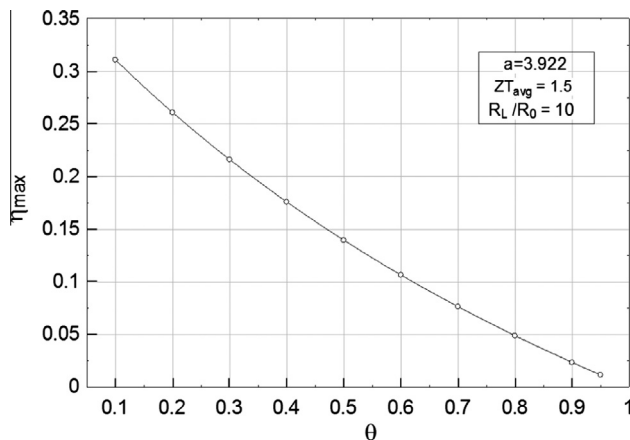


Fig. 5. Variation of maximum thermal efficiency with dimensionless temperature ratio for external load ratio of  $R_L/R_0 = 10$ .

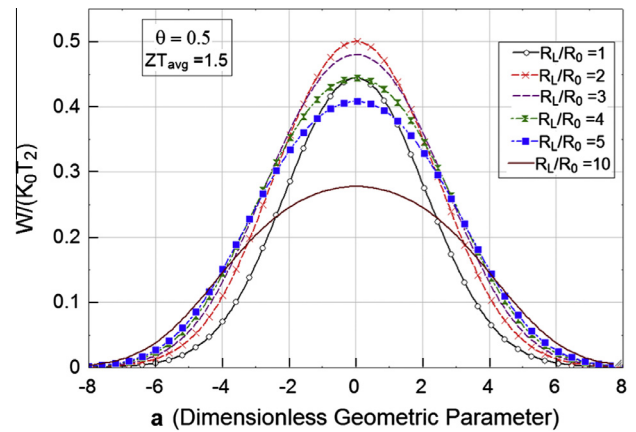


Fig. 6a. Variation of dimensionless output power with dimensionless geometric parameter ( $a$ ) for different values of external load ratio ( $R_L/R_0$ ) and temperature ratio  $\theta = 0.5$ .

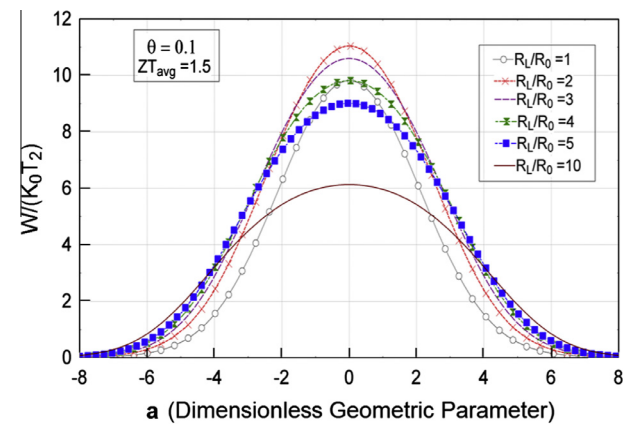


Fig. 6b. Variation of dimensionless output power with dimensionless geometric parameter ( $a$ ) for different values of external load ratio ( $R_L/R_0$ ) and temperature ratio  $\theta = 0.1$ .

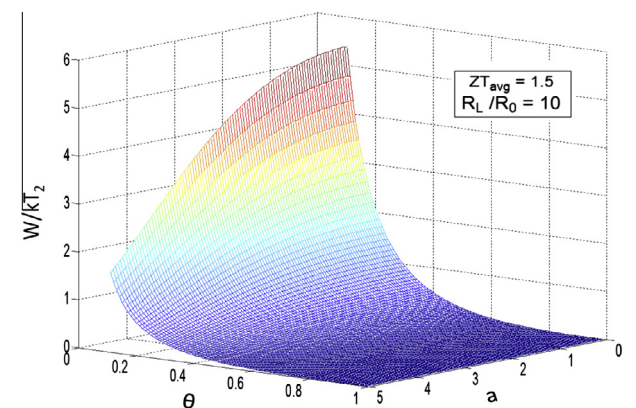


Fig. 7. Variation of dimensionless power output with dimensionless geometric parameter and dimensionless temperature for external load ratio of  $R_L/R_0 = 10$ .

Fig. 6 shows dimensionless power ( $W/K_0 T_2$ ) with geometric leg parameter for various values of external load ratio while Fig. 7 shows three-dimensional view of dimensionless power with geometric leg parameter and dimensionless parameter. Dimensionless power attains its maximum value for geometric leg parameter  $a = 0$  and it decays almost exponentially with increasing/decreasing

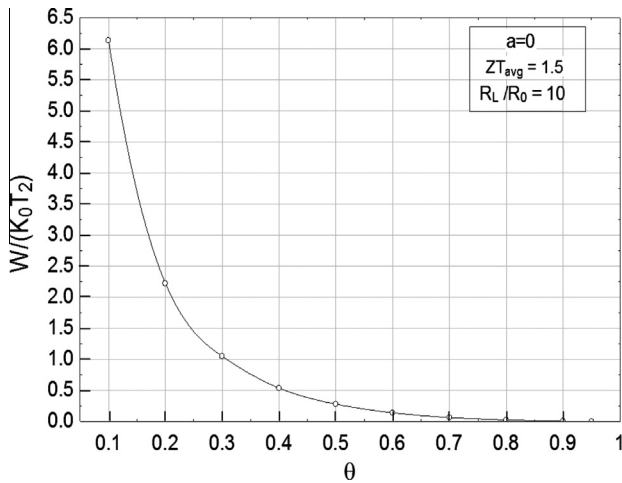


Fig. 8. Variation of maximum dimensionless output power with temperature ratio for external load ratio of  $R_L/R_0 = 10$ .

ing values of  $a$ . This behavior is attributed to the influence of geometric leg parameter on the device output (Eq. (29)), since the geometric leg parameter is associated with the leg resistance ( $R$ ). In this case, the maximum output power is inversely proportional to the leg resistance, i.e. reducing leg resistance results in increasing device output power. In addition, the influence of external load ratio on the device output power is in a nonlinear form. Consequently, the maximum power increases to reach its peak value for external load parameter of  $R_L/R_0 = 2$ . Moreover, further increase in external load parameter causes decay of the magnitude of the maximum output power. This nonlinear behavior can also be observed from Eq. (29). The value of the maximum output power increases with reducing temperature ratio ( $\theta$ ). It should be noted that reducing temperature ratio increases temperature difference across the device legs. This, in turn, increases both thermal efficiency and output power, since the Carnot efficiency of the device improves for low values of temperature ratio. This can be observed from Fig. 8, in which output power with temperature ratio is shown for external load ratio of  $R_L/R_0 = 10$ . This behavior is also seen from three-dimensional view of device output power variation as shown in Fig. 7. The geometric leg parameter resulting in the maximum efficiency does not yield the maximum device output power. This indicates that the occurrence of the maximum thermal efficiency does not correspond to the occurrence of the maximum output power. This can be seen from Fig. 9, in which

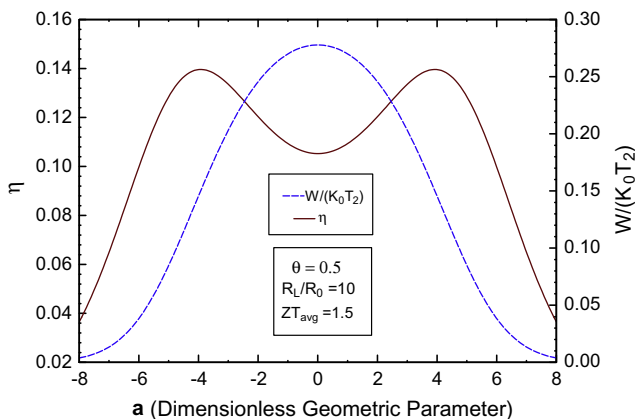


Fig. 9. Variation of efficiency and dimensionless output power with geometric leg parameter ( $a$ ) for external load ratio of  $R_L/R_0 = 10$ .

variation of thermal efficiency and output power of the device with geometric leg parameter is shown for external load ratio  $R_L/R_0 = 10$ . This situation also varies for different values of the external load ratio. Hence, when operating the device the care must be taken to secure the maximum output power with the highest corresponding thermal efficiency of the device. The operating parameters, therefore, are closely associated with the geometric features of the device legs. Although temperature ratio has significant effect on thermal efficiency and output power of the device, this effect does not change for different configuration of leg geometric parameter. Consequently, external load ratio is closely associated with thermal efficiency and output power. In this case, variation of the external load ratio requires alteration of geometric configuration of the device legs to achieve the maximum thermal efficiency or the maximum output power of the device.

#### 4. Conclusions

Influence of geometric configuration of thermoelectric power generator legs on thermal efficiency and output power of the device is investigated. Thermodynamic analysis is presented to formulate the device performance characteristics. The operating parameters including external load ratio ( $R_L/R_0$ ) and temperature ratio ( $\theta$ ) are incorporated in the analysis. A computer code is developed to simulate and demonstrate the effect geometric leg parameter on thermal efficiency and output power of the device for a bismuth telluride ( $\text{Bi}_2\text{Te}_3$ ) power generator. It is found that geometric leg parameter influence significantly device thermal efficiency which is more pronounced with external load ratio ( $R_L/R_0$ ). Increasing external load ratio enhances thermal efficiency of the thermoelectric generator; in which case, varying external load ratio modifies the value of corresponding geometric leg parameter for the maximum thermal efficiency. Thermoelectric device parallel pin geometry ( $a = 0$ ) results in the maximum thermal efficiency for low values of external load ratio. As the external load ratio increases, the corresponding leg geometric parameter becomes  $a > 0$  or  $a < 0$  for the maximum thermal efficiency. Reducing temperature ratio enhances the Carnot efficiency of the thermoelectric device. This, in turn, enhances thermal efficiency of the device; however, the influence of temperature ratio on leg geometric parameter maximizing thermal efficiency is insignificant. The maximum output power of the thermoelectric device takes place at  $a = 0$ , which corresponds to the parallel leg geometry of the device, for all values of external load ratio. The influence of external load ratio on the device output power is significant; in which case, increasing external load parameter first increases output power and further increase in external load ratio lowers the device output power. Temperature ratio influence significantly the magnitude of the device output power; in this case, reducing temperature ratio enhances output power. The occurrence of the maximum thermal efficiency does not correspond to the occurrence of the device maximum output power for a specific value of geometric leg parameter. Consequently, a care must be taken to select external load parameter such that thermal efficiency remains the maximum while output power is high during the operation for a given geometric leg configuration.

#### Acknowledgments

The authors would like to acknowledge the support provided by King Abdulaziz City for Science and Technology (KACST) through the Science and Technology Unit at King Fahd University of Petroleum and Minerals (KFUPM) for funding this work through project No. 09-ENE779-04 as part of the National Science, Technology and Innovation Plan.

## References

- [1] Hodes M. Optimal pellet geometries for thermoelectric power generation. *IEEE Trans Comp Pack* 2010;33(2):307–18.
- [2] Yilbas BS, Sahin AZ. Thermoelectric device and optimum external load parameter and slenderness ratio. *Energy* 2010;35(12):5380–4.
- [3] Lavric ED. Sensitivity analysis of thermoelectric module performance with respect to geometry. *Energy* 2010;21:133–8.
- [4] Sahin AZ, Yilbas BS, Shuja SZ, Momin O. Investigation into topping cycle: thermal efficiency with and without presence of thermoelectric generator. *Energy* Jul 2011;36(7):4048–54.
- [5] Xiao H, Gou X, Yang C. “Simulation analysis on thermoelectric generator system performance”, 2008 Asia Simulation Conference – 7th International Conference on System Simulation and Scientific Computing, ICSC 2008. 2008: 1183–1187.
- [6] Vatcharasathien N, Hirunlabh J, Khedari J, Daguenet M. Design and analysis of solar thermoelectric power generation system. *Int J Sust Energy* 2005;24(3):115–27.
- [7] Suzuki RO, Tanaka D. Mathematical simulation of thermoelectric power generation with the multi-panels. *J Power Sources* 2003;122(2):201–9.
- [8] Gou X, Heng X, Yang S. Modeling, experimental study and optimization on low-temperature waste heat thermoelectric generator system. *Appl Energy* 2010;87:3131–6.
- [9] Amatya R, Ram RJ. Solar thermoelectric generator for micropower applications. *J Electron Mater* 2010;39(9):1735–40.
- [10] Weinberg FJ, Rowe DM, Min G, Ronny PD. “On thermoelectric power conversion from heat recirculating combustion systems,” Proceedings of the Combustion Institute, Twenty-ninth International Symposium on Combustion Hokkaido University Sapporo Japan. 2002.
- [11] Freunek M, Müller M, Ungan T, Walker W, Reindl LM. New physical model for thermoelectric generators. *J Electron Mater* 2009;38(7):1214–20.
- [12] Yamashita O. Effect of linear temperature dependence of thermoelectric properties on energy conversion efficiency. *Energy Convers Manage* 2008;49(11):3163–9.
- [13] Yamashita O. Effect of linear and non-linear components in the temperature dependences of thermoelectric properties on the energy conversion efficiency. *Energy Convers Manage* 2009;50(8):1968–75.
- [14] Domenicali CA. Irreversible thermodynamics of thermoelectricity. *Rev Modern Phys* 1954;26(2):237–75.
- [15] Hadjistassou C, Kyriakides E, Georgiou J. Designing high efficiency segmented thermoelectric generators. *Energy Convers Manage* 2013;66:165–72.
- [16] Landecker K. On power-generating thermojunctions with radial flow of current. *Solar Energy* 1977;19(5):439–43.
- [17] Lesage FJ, Pelletier R, Fournier L, Sempels ÉV. Optimal electrical load for peak power of a thermoelectric module with a solar electric application. *Energy Convers Manage* 2013;74:51–9.
- [18] Riffat SB, Qiu GQ. Design and characterization of a cylindrical, water-cooled heat sink for thermoelectric air-conditioners. *Int J Energy Res* 2006;30(2):67–80.
- [19] Clingman WH. Entropy production and optimum device design. *Adv Energy Convers* 1961;1(C):61–79.
- [20] Semenyuk VA. Efficiency of cooling thermoelectric elements of arbitrary shape. *J Eng Phys* 1977;32(2):196–200.
- [21] Lesage FJ, Sempels ÉV, Lalande-Bertrand N. A study on heat transfer enhancement using flow channel inserts for thermoelectric power generation. *Energy Convers Manage* 2013;75:532–41.
- [22] Lossec M, Multon B, Ben H. Ahmed, Sizing optimization of a thermoelectric generator set with heat sink for harvesting human body heat. *Energy Convers Manage* 2013;68:260–5.
- [23] Landecker K. Some aspects of the performance of refrigerating thermojunctions with radial flow of current. *J Appl Phys* 1976;47(5):1846–51.
- [24] Antonio A, Jorge V, Rafael P. “Performance analysis of thermoelectric pellets with non-constant cross sections”, Proceedings of the 7th European Workshop on Thermoelectrics.
- [25] Thacher EF. “Shapes which maximise thermoelectric generator efficiency”, Proc 4th International Conference on Thermoelectric, Energy Conversion. pp. 67–74, 1982.
- [26] Bejan A, Lorente S. Design with constructal theory. New York: John Wiley and Sons; 2008.
- [27] Sahin AZ, Yilbas BS. Thermodynamic irreversibility and performance characteristics of thermoelectric power generator. *Energy Apr* 2013:1–6.
- [28] Sahin AZ, Yilbas BS. The thermoelement as thermoelectric power generator: effect of leg geometry on the efficiency and power generation. *Energy Convers Manage* 2013;65:26–32.